Contrasting synoptic weather patterns between non-dust high particulate matter events and Asian dust events in Seoul, South Korea

Myung-Il Jung[a], Seok-Woo Son[a,*], Hyun Cheol Kim[b,c], Sang-Woo Kim[a], Rokjin J. Park[a] and Deliang Chen[d]

[a]School of Earth and Environmental Sciences, Seoul National University, Seoul, 08826, South Korea

[b]Air Resources Laboratory, National Oceanic and Atmospheric Administration, College Park, MD, 20740, USA

[c]Cooperative Institute for Climate and Satellites, University of Maryland, College Park, MD, 20740, USA

[d]Regional Climate Group, Department of Earth Sciences, University of Gothenburg, Gothenburg, Sweden

Apr. 2019

*Corresponding author: Seok-Woo Son, School of Earth and Environmental Sciences, Seoul National University, 1 Gwanak-ro, Gwanak-gu, Seoul, 08826, South Korea

E-mail: seokwooson@snu.ac.kr

Abstract

The serious degradation of regional air quality is a critical social issue in East Asia despite continuous efforts to reduce the emission of pollutants and their precursors. To better understand high-pollution events in this region, the synoptic weather patterns associated with springtime non-dust high PM_{10} (HPM) events and Asian dust (AD) events in Seoul, South Korea, are examined for the 2001-2018 period. While HPM events are associated with weak surface cyclonic circulations over the Southeast China, AD events are characterized by strong cyclones over Northeast China. Composite weather maps show that mid-tropospheric circulation anomalies are exactly the opposite between the two events with anticyclonic anomalies over the Korean Peninsula for HPM events and cyclonic anomalies for AD events. The cluster analyses further reveal that HPM events are not determined by a single dominant weather pattern. The HPM events are associated with surface cyclonic circulations from southeastern China to the Sea of Okhotsk or anticyclonic circulations around the Korean Peninsula, accounting for transboundary pollution transport from China and regional stagnation of pollutants, respectively. This result is in contrast with the AD events which are primarily driven by vertically well-organized continental cyclones.

Keywords: High PM_{10} events, Asian dust events, Synoptic weather patterns, Self-organizing map (SOM) analysis

1. Introduction

With the acceleration of urbanization and industrialization in recent decades, the problem of air pollution in East Asian megacities has been addressed since the 2000s (Wang et al., 2014; Wang and Chen, 2016; Nam et al., 2018). In particular, fine dusts, that include both particulate matters (PMs) with diameters of less than or equal to 10 μm (PM_{10}) and 2.5 μm ($PM_{2.5}$), have recently received significant attention due to their adverse effects on human health, visibility, and climate (Zheng et al., 2015; Lu et al., 2017; Corrigan et al., 2018). Although the trend of PM concentration has decreased in the 2000s due to government regulations such as emission restrictions, East Asia still suffers from the frequent occurrence of high PM events (Kim et al., 2017b).

Regional air quality in East Asia is closely related to local emissions from both natural and anthropogenic sources (Hu et al., 2015; Chen et al., 2017; Ryou et al., 2018). It is also affected by the long-range transport of natural dusts and anthropogenic aerosols (Zhang et al., 2016; Kim et al., 2017a; Yu et al., 2019). The possible sources and pathways of PMs in Seoul, South Korea, are described in Fig. 1. The PM_{10} concentration in Seoul, especially on highly polluted days, is influenced by the long-range transport from industrialized regions in eastern China as well as the arid regions in northern China and Mongolia (Chung et al., 2014; Wang et al., 2018). Among them, the transboundary transport of PMs from China to South Korea is a critical issue when PMs are trapped over Seoul (green arrow in Fig. 1). Such transport differs from the long-range transport of natural dusts from the desert (brown arrow in Fig. 1). Chung et al. (2014) showed that the source regions and transport mechanisms are quite different in these two episodic PM transportations.

Natural dust events, which are often referred to as Asian dust events, frequently occur in Seoul during the dry season (Kim et al., 2008; Ahmed et al., 2015). The dusts mainly originate from arid regions, such as the Gobi Desert and Inner Mongolia and are transported downstream by strong background winds. These events are frequently observed, especially when the dust source region is dry and the surface wind is sufficiently strong to float dust particles from the surface (Kang et al., 2011; Shao et al., 2011). This strong surface wind is typically related to the migratory cyclone, which occurs frequently in spring (Takemi and Seino, 2005; Cho et al., 2018). Furthermore, during transportation over East Asia, natural dusts can be mixed with suspended pollutants from anthropogenic sources, which changes their optical properties and chemical composition (Sun et al., 2005; Shin et al., 2015; Wang et al., 2018).

Unlike Asian dust (AD) events, the sources and pathways of non-dust high PM (HPM) events are not fully understood, although there are several studies describing possible causes of HPM events (Liang et al., 2016). The relative importance of local emissions versus transboundary transport, for instance, is not well quantified. It is also unclear how transboundary transport is organized according to the weather pattern. By presenting backward trajectory results of high PM_{10} days in Seoul, Lee et al. (2011) reported that high PM_{10} episodes in Seoul are influenced by both internal and external sources, inferring that the latter occurs approximately twice as frequently as the former. Oh et al. (2015) further suggested that multi-day pollution episodes are favorable in Seoul when air pollutants emitted in eastern China are trapped within the boundary layer through strong anticyclonic circulation. The widespread anticyclonic anomalies in the mid-troposphere from over eastern China to Korea are suggested as the key condition for long-lasting high PM_{10} episodes in Seoul. The omega-shaped blocking and almost stationary atmospheric pattern may also provide favorable conditions for high PM concentrations in Seoul (Seo et al., 2017). However, a characterization of the synoptic weather patterns associated with HPM events and their difference from AD events are still not well reported.

The purpose of the present study is to identify the synoptic weather patterns associated with HPM events and AD events in Seoul. The seasonal cycle and temporal variability in HPM events are documented by analyzing long-term PM_{10} observations in the Seoul metropolitan region. Then, the associated meteorological fields are examined with an emphasis on the vertical coupling between the surface and tropospheric circulations. To determine the robustness of the weather pattern derived from the composite analysis, a cluster analysis is also conducted. All analyses are separately performed for HPM and AD events. A direct comparison between HPM and AD events reveals a distinct difference in their synoptic weather patterns.

In the following section, the data and analysis methods are introduced. Section 3 describes the results of the composite analysis and clustering analysis. Finally, a summary and conclusions are presented in Section 4.

2. Data and methods

2.1. Data

Two independent observational datasets are used to define the high-pollution events in Seoul during the last 18 years (2001–2018). These are daily PM_{10} data from the Ministry of Environment (MOE; https://www.airkorea.or.kr) in Korea and AD days reported by the Korean Meteorological Administration (KMA; https://www.kma.go.kr). To minimize possible measurement errors and to avoid influence of local scale variability which not the focus of this study, the PM_{10} concentrations, measured by the beta-ray absorption method, are simply averaged across 25 air quality monitoring stations in the Seoul metropolitan region (MOE, 2018). AD events are simple to obtain from KMA. The KMA announces the AD dates by considering the movement of desert dust, abrupt changes in local PM_{10} concentration and direct visual identification (Lee et al., 2013).

The synoptic weather patterns, based on 6-hourly meteorological data, are obtained from the Japanese 55-year Reanalysis (JRA-55; Kobayashi et al., 2015). These data are converted into daily-mean data by considering the local standard time in Korea. The variables of interest are sea level pressure (SLP), geopotential height (Z), and horizontal/vertical winds with a spatial resolution of 2.5˚ latitude by 2.5˚ longitude with 17 pressure levels. As synoptic circulations have significant seasonality, most analyses are conducted for anomaly fields with the daily climatology removed.

2.2. High PM_{10} (HPM) and Asian dust (AD) events

Two types of high-pollution events, i.e., non-dust high PM_{10} (HPM) events and Asian dust (AD) events, are defined in this study. The days with a daily-mean PM_{10} concentration greater than 100 μg m^{-3}, corresponding to the environmental standard of the ambient air quality in South Korea (MOE, 2018), are selected as high PM_{10} days. Among these dates, the days of non-dust events are subsampled by removing KMA-defined AD days. Consecutive days with high PM_{10} concentrations exceeding 100 μg m^{-3} are considered to be a single event, and the maximum PM_{10} concentration day is set as the central day. To avoid double counting, each HPM event is set as at least three days apart from another.

Based on these criteria, a total of 146 HPM events and 67 AD events were detected for the 2001-2018 period. Specifically, 40 and 67 HPM events are identified in spring (March–May; MAM) and winter (November–February; NDJF), respectively. This is because high-pollution events are more frequent in these seasons. Likewise, 46 and 20 AD events are detected in spring and winter, respectively.

2.3. Composite analysis

The time evolution of synoptic weather patterns, associated with HPM and AD events, are examined with composite weather maps in daily intervals from 2 days before and to the central day of each event. The analysis domain is set to the East Asia region (20˚-60˚N, 90˚-150˚E) to account for both local emissions and long-range transport (Fig. 1). The vertical structure of atmospheric circulation is also examined from 1000 hPa to 500 hPa, focusing on the lower- to mid-troposphere.

In all analyses, the statistical significance is tested by conducting a two-tailed Student's t-test with a null hypothesis of a zero population mean. The degree of freedom is determined by assuming that each event is independent.

2.4. Cluster analysis

The self-organizing map (SOM) analysis (Kohonen, 2001) is conducted to cluster weather patterns associated with HPM and AD events. The SOM works by reducing multiple weather maps into several representative patterns in physical space, assuming non-linearity of datasets through iterative training. After completion of a sufficient training process, each weather map is assigned to the optimal cluster with the best matching unit. See the appendix of Johnson et al. (2008) for a detailed description of the SOM analysis. The patterns classified by this method have been used to understand meso-scale precipitation patterns (e.g., Jo et al. 2019) and synoptic-scale atmospheric circulation patterns (e.g., Horton et al., 2015; Huang et al., 2017). For example, by applying the SOM method to the daily SLP anomaly fields, Johnson et al. (2008) characterized various teleconnection patterns in association with the North Atlantic Oscillation.

One of the key parameters that need to be specified in the SOM analysis is the number of nodes (or clusters). When too many nodes are used, some clusters could become similar and eventually have low compressibility. If the number of nodes is too small, dissimilar maps could be assigned into the same cluster, which could result in inaccurate clustering (Johnson et al., 2008). Using the daily SLP anomaly fields at the central date of each event as input data, a series of sensitivity tests were conducted with varying SOM array sizes (not shown). The East Asian region around the Korean Peninsula (20˚-60˚N, 100˚-140˚E) is selected as the SOM analysis domain. By considering both compressibility and accuracy, three nodes with a 1×3 array are chosen as the optimal size for both HPM and AD events. Although not shown, the overall results are not strongly sensitive to the details of the array (e.g., four nodes with a 2×2 array).

3. Results

3.1. HPM and AD events in Seoul

Figure 2a shows the seasonal cycle of the number of HPM and AD events in Seoul. The HPM events (red bar) exhibit a gradual seasonality with maximum and minimum frequencies in January and August, respectively. The winter maximum is likely caused by high emissions under dry and stagnant weather conditions. In contrast, the summer minimum is mainly due to the washout effect of monsoon precipitation in late June to August (Wang et al., 2015; Cheng et al., 2016) and that of typhoon-related precipitation in late summer (Liu et al., 2018).

It is also noteworthy that the number of HPM events (red bars) is relatively smaller in April than in March and May. Such sub-seasonal variation, which also appears in the total number of HPM days, can be partly related to more frequent precipitation in April than in March and a stronger surface wind in April than in May (not shown). Note that a strong surface wind could enhance the vertical mixing and ventilation of pollutants. Accordingly, the PM_{10} concentration in Seoul is negatively correlated with the local wind speed (Kim et al., 2017b).

Unlike HPM events, AD events (blue bars) are noticeably more frequent during springtime (March to May) than during other seasons. AD events are not observed from June to September. Even during winter, when HPM events are frequent, AD events occur much less often than in spring. This seasonal cycle, characterized by predominant AD events in spring, is determined not only by surface conditions and sufficiently strong surface winds in dust source regions (i.e., the Gobi Desert and Inner Mongolia; Fig. 1), but also by wind directions that can transport the dust to downstream (Qian et al., 2002; Takemi and Seino, 2005). Here, a strong surface wind is typically caused by a migratory cyclone in northern China. As shown in Penny et al. (2010) and Cho et al. (2018), a synoptic-scale cyclone, which can lift desert dusts and often carry them downstream, is the most active during spring in this region. Although surface wind is also sufficiently strong in winter, dust source regions are frozen or partly covered by snow, preventing dust erosion (Nandintestseg and Shinoda, 2011).

Figures 2b and c illustrate the long-term changes of HPM and AD events for the spring (MAM) and winter seasons (NDJF). The number of springtime HPM events has slightly decreased with a significant trend of -0.18 ± 0.17 events year^{-1} since 2003 (red bars), or an insignificant trend of -0.15 ± 0.15 events year^{-1} since 2001. A decline in HPM events is also found in wintertime with -0.31 ± 0.18 events year^{-1} over the analysis period.

Kim et al. (2017b) mentioned that the overall decrease in PM_{10} concentrations in Seoul is caused by the emission control efforts of the Korean government and neighboring countries. Nevertheless, high-pollution events still occur, such as during the 2013/2014 winter. Such events are likely caused by relatively weak atmospheric circulations that enhance the accumulation of PM_{10} concentrations emitted from local sources.

The blue bars in Fig. 2b denote the number of springtime AD events with a significant declining trend (-0.16±0.13 events year^{-1}). Only two or fewer AD events have been reported since 2009, except for 2011 and 2015. This trend is quite similar to the frequency change in HPM events. The wintertime AD events, however, show essentially no trend during the analysis period (blue bars in Fig. 2c). A pronounced interannual variability is evident with relatively frequent AD events during winters from 2007/08 to 2010/11. This variability is likely caused by the hydro-climate variability in dust source regions and dust transport to the Korean Peninsula although the exact mechanism remains to be determined.

The above results suggest that HPM and AD events have different temporal characteristics with different seasonal cycles and long-term variabilities. In fact, their interannual variabilities are not correlated. Even in spring, when both HPM and AD events frequently occur, their occurrence frequencies (i.e., the red and blue bars in Fig. 2b) are not correlated with each other.

Figure 3 further shows that the daily evolution of PM_{10} concentration differs between HPM and AD events. The PM_{10} concentration of HPM events nearly doubled from lag -2 day to the central day (lag 0 day). On average, the maximum concentration reaches 122.3 µg m-3 in spring and 133.5 µg m-3 in winter (Fig. 3a). The PM_{10} concentration of AD events rapidly increases during the two days (more than three times). Although relatively comparable to HPM events at lag -2 days, a maximum PM_{10} concentration at the AD central day often exceeds 224.9 µg m-3 in spring and 186.9 µg m-3 in winter (Fig. 3b). Note that the springtime AD events have a higher PM_{10} concentrations than the wintertime events. This finding is different from that of the HPM events which show a slightly higher concentration in winter than in spring.

3.2. Composite analyses

Do synoptic weather patterns differ between HPM and AD events? Below, the three dimensional atmospheric circulation patterns during HPM and AD events are compared. Only the spring season is considered, which is when the numbers of HPM and AD events are comparable. As shown in the supplementary material, the overall results do not change much during winter.

Figure 4a presents the seasonal-mean SLP and 925-hPa wind fields. A weak westerly of less than 5 m s^{-1} is prevalent around Seoul (denoted in a red triangle), which results from a cyclonic circulation in the northeast and an anticyclonic circulation in the southern of the Korean Peninsula. Under this weak background flow, anomalous winds become comparable to or even stronger than the climatological winds (Figs. 4b-g).

Figures 4b-d illustrate the temporal evolutions of SLP and 925-hPa wind anomalies from lag -2 day to the central day, which are associated with HPM events. The negative SLP anomaly, located over Mongolia at lag -2 day, rapidly moves southeastward and reaches southeastern China on the central day. This system, however, is not well organized and decays over time (Fig. 4b). Although statistically insignificant, the associated wind anomalies are southerlies around the Korean Peninsula (Fig. 4d). By considering climatological winds, the total winds are weak southwesterlies. These winds may provide favorable conditions for pollutant transport from the industrial regions of eastern China to Korea.

The cyclonic anomalies shown in Figs. 4b-d, are vertically shallow and confined to near the surface without significant wind anomalies in the upper level (Figs. 5b-d). Positive geopotential height anomalies are observed at the 500-hPa level (e.g., Fig. 5d), unlike the negative SLP anomalies over the region (e.g., Fig. 4d). Moreover, although the surface system weakens over time, the mid-tropospheric anomalies become stronger as they slowly travel southeastward to Seoul. These contrasting features between the surface and mid-troposphere clearly indicate that circulation anomalies associated with HPM events are not well organized in the vertical direction.

As Figs. 4e-g and 5e-g show, identical analyses are also conducted for AD events. A well-developed cyclone, passing through the arid regions of Mongolia and northern China (Fig. 4e) and traveling eastward over time (Figs. 4f-g), is evident. At lag -2 day, the near-surface wind speed over northern China is up to 10 m s^{-1} (sum of Figs. 4a and e) which could trigger wind erosion over the Gobi Desert and Inner Mongolia especially along the cold front of the developing cyclone (Takemi and Seino, 2005). Then, the lifted dust could be transported downstream with the cyclone and westerly belt (Ghim et al., 2017).

Here, it should be highlighted that the surface cyclone during AD events is well organized in the vertical direction. As shown in Figs. 5e–g, the cyclonic anomaly in the mid-troposphere, which develops over time, is well coupled with the surface cyclone; they travel with similar speeds and directions.

These results indicate that the overall weather patterns associated with HPM and AD events are different. While the HPM events are accompanied by a weak cyclone over eastern China, AD events are associated with a well-developed continental cyclone over the northeast of the Korean Peninsula. These weather patterns lead to nearly opposite near-surface wind anomalies over Seoul; i.e. anomalous southwesterlies during HPM events but northwesterlies during AD events (comparing Figs. 4d with g). The difference between HPM and AD events is even clearer in the mid-troposphere where opposite signs of geopotential height anomalies are found (compare Figs. 5d with g). These anomalies intensify over time as they travel toward Seoul.

Figure 6 further depicts the difference in vertical structures between HPM and AD events. The geopotential height and wind anomalies that are averaged over 35˚-40˚N, which is centered at Seoul, are shown in the longitude-pressure domain. Here, the vertical motion is represented by the reversed p-velocity multiplied by the aspect ratio. The circulation anomalies associated with HPM events develop in the mid- to upper-troposphere and then extend downward over time (Figs. 6a-c). Unlike the positive geopotential height anomalies in the upper level, the negative anomalies in the western Seoul are at a maximum near the surface (Figs. 6b and c). Although vertical motions accompany weak updrafts, they are negligibly weak around Seoul on the central day (Fig. 6c).

The circulation anomalies associated with AD events are characterized by negative geopotential height anomalies near the surface, and these anomalies extend slightly upward over time (Figs. 6d-f). Vertical motion around Seoul is dominated by a downdraft on the backside of the surface cyclone on the central day (Fig. 6f). This circulation pattern, i.e., anomalous westerlies in the mid-troposphere (Fig. 6d) and downdraft below (Fig. 6f), likely favors the eastward transport of natural dust to the Korean Peninsula.

3.3. Cluster analyses

The above results indicate that HPM and AD events are associated with different weather patterns. However, the composite maps do not necessarily represent all events, although they are statistically significant. To evaluate the robustness of the composite maps, SLP and 500-hPa geopotential height anomalies averaged over the boxed regions in Figs. 4 and 5 are examined for individual cases (Fig. 7). Consistent with the composite maps, the majority of HPM events are characterized by negative SLP and positive 500-hPa geopotential height anomalies (Fig. 7a). However, the spreads of these events are substantially large and only 52.5% of HPM events are distributed in the upper-left quadrant. More importantly, the correlation of the two variables is not statistically significant.

The SLP and geopotential height anomalies are well defined among AD events. Approximately 70 % of AD events are accompanied by cyclonic anomalies from the surface to 500 hPa (lower-left quadrant of Fig. 7b). The SLP anomalies are significantly correlated with 500-hPa geopotential height anomalies. These results indicate that while HPM events occur under various meteorological conditions, most AD events are driven by continental cyclones which are well organized in the vertical direction.

3.3.1. SOM clusters for HPM events

To better understand the varying synoptic weather patterns associated with HPM events (Fig. 7a), HPM events are further classified into three subgroups using the SOM method. Figure 8 presents the synoptic patterns of all clusters in terms of 500-hPa geopotential height, SLP, and 925-hPa wind anomalies. The three clusters consist of 14, 15, and 11 HPM events, respectively. Each cluster shows a distinct weather pattern, implying that the composite maps represent a mixture of different weather patterns (Figs. 4d and 5d).

Cluster 1 of HPM events is characterized by strong cyclonic SLP anomalies over the Sea of Okhotsk on the central day (Fig. 8b). As a result, strong southwesterlies are prevalent around Seoul. In the mid-troposphere, weak anticyclonic anomalies appear over Japan and the East Sea (or Sea of Japan), with negative anomalies over the Sea of Okhotsk, resulting in an enhanced westerly jet. Note that the direction of surface winds over eastern China does not favor the accumulation of PM_{10} concentration in Seoul. Instead, these winds can effectively carry pollutants from upstream source regions. Although not shown, cyclonic anomalies in this cluster are formed downstream of the Altai-Sayan Mountains and travel eastward over time. This result suggests that the HPM events in this cluster are partly related to the transboundary pollution transport from the industrial regions of eastern China to Korea.

In contrast to cluster 1, the surface weather pattern of cluster 3 is dominated by anticyclonic anomalies over broad regions spanning from Mongolia to Japan (Fig. 8f). The weak positive anomalies around Japan are well connected with anticyclonic anomalies in the free atmosphere (Fig. 8e). Considering that anticyclonic circulation leads to a calm atmosphere and downdraft, this condition may facilitate the accumulation of local pollutants. Note from Figs. 8e and f that wind anomalies nearly offset the climatological northwesterlies in the both mid-troposphere and near surface (comparing Figs. 5a and 4a). The anomalies cause stagnant conditions over the Korean Peninsula as discussed in Lee et al. (2011) and Oh et al. (2015).

Figures 8c and d present cluster 2. This cluster seems to be a mixture of clusters 1 and 3 with cyclonic anomalies over northern China and anticyclonic anomalies over Japan. Near-surface winds around Seoul are close to climatological winds, making synoptic weather patterns difficult to interpret. In the mid-troposphere, strong anticyclonic circulation anomalies appear over the northern part of the Korean Peninsula. This result is consistent with previous studies which suggest that positive 500-hPa geopotential height anomalies are associated with the accumulation of local pollutants (Lee et al., 2011; Oh et al., 2015).

As earlier addressed, one of the key features of spring synoptic weather systems in East Asia is the routine passage of migratory cyclones and anticyclones. These systems, which are evident in clusters 1 and 3, likely affect the PM_{10} concentration in Seoul in different ways. The cyclonic system on the west of the

Korean Peninsula provides a feasible condition for pollution transport from eastern China to Korea. On the other hand, the presence of an anticyclonic system on the eastern Korean Peninsula could facilitate the accumulation of locally emitted pollutants.

3.3.2. SOM clusters for AD events

Figures 4 and 5 show that the continental cyclone within 40˚-50˚N, corresponding to the baroclinic frontal zone, is responsible for AD events. This cyclone appears in all clusters (Fig. 9) with varying spatial scales. The area of the cyclonic anomaly in cluster 1 is relatively broad, covering northern China to Japan (Fig. 9b), whereas a synoptic-scale cyclone centered over eastern Japan is well defined in cluster 2 (Fig. 9d). The cyclonic anomaly in cluster 3 is weak and has a rather small spatial scale (Fig. 9f). In the mid-troposphere, all clusters exhibit strong cyclonic anomalies around the Korean Peninsula.

In cluster 1, which explains 15 events, the broad region of cyclonic anomalies tends to expand southeastward over time (Fig. 9b). Although not shown, this circulation pattern reaches the maximum intensity one day before the central day, and accompanies anomalous westerlies from the surface to the mid-troposphere around Seoul. Under this condition, not only desert dust but also industrial pollutants over Northeast China could affect PM_{10} concentrations in Seoul.

The near-surface cyclones in clusters 2 and 3, which are located over Japan, show different development stages. In cluster 2, the continental cyclone tends to increase (or at least maintain) its spatial scale as the cyclone travels eastward, reaching its maximum intensity on the central day (Fig. 9d). However, the cyclone in cluster 3 is rather weak (Fig. 9f), even though the circulation anomaly is well defined in the mid-troposphere as in cluster 2 (Fig. 9e). Although not shown, this cyclone becomes weaker from lag -2 day to the central day, implying that the cluster-3 AD events are associated with slightly decaying cyclones.

These results confirm that most AD events are caused by migratory continental cyclones. A subtle difference among AD events could be explained by the different spatiotemporal scales and the developmental stages of individual cyclones. Notably, the variability among AD-event clusters is far smaller than that among HPM-event clusters. All AD-event clusters are characterized by synoptic-scale cyclones to the east or northeast of Seoul with a similar vertical structure. This similarity contrasts with the diverse synoptic weather patterns associated with HPM events (comparing Figs. 8 with 9).

4. Summary and conclusions

In this study, we examined the synoptic weather patterns when high PM_{10} concentrations are observed in Seoul, South Korea, over the past 18 years (i.e., 2001-2018). Two types of high PM_{10} events, non-dust high PM events (i.e., HPM events) and Asian dust events (i.e., AD events), are identified, and associated synoptic weather patterns of these two events are compared. The key findings are summarized as follows.

First, both HPM and AD events exhibit a distinct seasonal cycle with a maximum occurrence frequency during the cold season but a distinct minimum during the summer Asian monsoon period. Both events are common in spring (March-May) with a weak hint of decreasing frequency over the last 18 years.

Second, the synoptic weather patterns during HPM and AD events are quite different. While HPM events accompany weak cyclonic anomalies that are mostly confined to the near surface, AD events are associated with strong cyclonic anomalies that are vertically well organized. As such, mid-tropospheric circulation anomalies are anticyclonic for HPM events but cyclonic for AD events. Consistent with previous findings (Kim et al., 2010; Park et al., 2013), strong continental cyclones, initiated over Mongolia, are firmly correlated with the occurrence of AD events in Seoul.

Third, the surface weather patterns associated with HPM events exhibit a considerable variation among the events. Based on SOM clustering, HPM events are classified into those associated with (i) cyclonic anomalies from Mongolia to the Sea of Okhotsk, (ii) anticyclonic anomalies around the Korean Peninsula, and (iii) a mixture of them. The cyclonic and anticyclonic anomalies likely provide favorable conditions for pollutant transport and the regional stagnation of pollutants, respectively.

Fourth, most AD events accompany a continental cyclone that approaches from northern China to the

Korean Peninsula. Differences among the events are mainly determined by the spatial scale and intensity of the cyclone.

In conclusion, this study demonstrates that synoptic weather patterns play an important role in regulating the air quality in Seoul. The detailed mechanisms, however, are not explored in this study. The physical and/or chemical processes, which are responsible for HPM and AD events, could be quantitatively addressed by integrating a numerical model (e.g., Kim et al., 2017a, 2017b). The model experiments with and without enhanced local emissions could be particularly useful to better understand the synoptic weather patterns leading to HPM and AD events in Seoul. Such modeling studies will be conducted in a future study.

Acknowledgments

This study was funded by the Korea Meteorological Administration Research and Development Program under Grant KMI2018-01112.

Conflicts of Interests

The authors declare no conflict of interest.

References

Ahmed, E., K.-H. Kim, Z.-H. Shon, and S.-K. Song, 2015: Long-term trend of airborne particulate matter in Seoul, Korea from 2004 to 2013. *Atmos. Environ.*, 101, 125-133. https://doi.org/10.1016/j.atmosenv.2014.11.024

Chen, W., D.Q. Tong, S. Zhang, X. Zhang, and H. Zhao, 2017: Local PM_{10} and $PM_{2.5}$ emission inventories from agricultural tillage and harvest in northeastern China. *J. Environ. Sci.*, 57, 15-23. https://doi.org/10.1016/j.jes.2016.02.024

Cheng, X., T. Zhao, S. Gong, X. Xu, Y. Han, Y. Yin, L. Tang, H. He, and J. He, 2016: Implications of East Asian summer and winter monsoons for interannual aerosol variations over central-eastern China. *Atmos. Environ.*, 129, 218-228. https://doi.org/10.1016/j.atmosenv.2016.01.037

Cho, H.-O., S.-W. Son, and D.-S.R. Park, 2018: Springtime extra-tropical cyclones in Northeast Asia and their impacts on long-term precipitation trends. *Int. J. Climatol.*, 38, 4043-4050. https://doi.org/10.1002/joc.5543

Chung, Y.S., H.-S. Kim, and Y. Chun, 2014: On large-scale transport of dust storms and anthropogenic dust-falls over east Asia observed in central Korea in 2009. *Asia-Pacific J. Atmos. Sci.*, 50, 345–354. https://doi.org/10.1007/s13143-014-0021-x

Corrigan, A.E., M.M. Becker, L.M. Neas, W.E. Cascio, and A.G. Rappold, 2018: Fine particulate matters: The impact of air quality standards on cardiovascular mortality. *Environ. Res.*, 161, 364-369. https://doi.org/10.1016/j.envres.2017.11.025

Ghim, Y.S., J.Y. Kim, and Y.-S. Chang, 2017: Concentration variations in particulate matter in Seoul associated with Asian dust and smog episodes. *Aerosol Air Qual. Res.*, 17, 3128-3140. https://doi.org/10.4209/aaqr.2016.09.0414

Horton, D.E., N.C. Johnson, D. Singh, D.L. Swain, B. Rajaratnam, and N.S. Diffenbaugh. 2015: Contribution of changes in atmospheric circulation patterns to extreme temperature trends. *Nature*, 522, 465-469. https://doi.org/10.1038/nature14550

Hu, J, L. Wu, B. Zheng, Q. Zhang, K. He, Q. Chang, X. Li, F. Yang, Q. Ying, and H. Zhang, 2015: Source contributions and regional transport of primary particulate matter in China. *Environ. Pollut.*, 207, 31-42. http://dx.doi.org/10.1016/j.envpol.2015.08.037

Huang, W., R. Chen, Z. Yang, B. Wang, and W. Ma, 2017: Exploring the combined effects of the Arctic Oscillation and ENSO on the wintertime climate over East Asia using self-organizing maps. *J. Geophys. Res. Atmos.*, 122, 9107-9129. https://doi.org/10.1002/2017JD026812

Jo, E., C.-I. Park, S.-W. Son, J.-W. Roh, G.-W. Lee, and Y.-H. Lee, 2019: Classification of localized heavy rainfall events in South Korea. *Asia-Pacific J. Atmos. Sci.*, submitted.

Johnson, N.C., S.B. Feldstein, and B. Tremblay, 2008: The continuum of Northern Hemisphere teleconnection patterns and a description of the NAO shift with the use of Self-Organizing Maps. *J. Climate*, 21, 6354–6371. https://doi.org/10.1175/2008JCLI2380.1

Kang, J.-Y., S.-C. Yoon, Y. Shao, and S.-W. Kim, 2011: Comparison of vertical dust flux by implementing three dust emission schemes in WRF/Chem. *J. Geophys. Res.*, 116, D09202. https://doi.org/10.1029/2010JD014649

Kim, H.C., E. Kim, C. Bae, J.H. Cho, B.-U. Kim, and S. Kim, 2017a: Regional contributions to particulate matter concentration in the Seoul metropolitan area, South Korea: seasonal variation and sensitivity to meteorology and emissions inventory. *Atmos. Chem. Phys.*, 17,10315-10332. https://doi.org/10.5194/acp-17-10315-2017

Kim, H.C., S. Kim, B.-U. Kim, C.-S. Jin, S. Hong, and R. Park, 2017b: Recent increase of surface particulate matter concentrations in the Seoul Metropolitan Area, Korea. *Scientific Reports*, 7, 4710. https://doi.org/10.1038/s41598-017-05092-8

Kim, S.-W, S.-C. Yoon, and J. Kim, 2008: Columnar Asian dust particle properties observed by sun/sky radiometers from 2000 to 2006 in Korea. *Atmos. Environ.*, 42, 492-504. https://doi.org/10.1016/j.atmosenv.2007.09.055

Kim, S.-W, S.-C. Yoon, J. Kim, J.-Y. Kang, and N. Sugimoto, 2010: Asian dust event observed in Seoul, Korea, during 29-31 May 2008: Analysis of transport and vertical distribution of dust particles from lidar and surface measurements. *Sci. Total Environ.*, 408, 1707-1718. https://doi.org/10.1016/j.scitotenv.2009.12.018

Kobayashi, S., Y. Ota, Y. Harada, A. Ebita, M. Moriya, H. Onoda, K. Onogi, H. Kamahori, C. Kobayashi, H. Endo, K. Miyaoka, and K. Takahashi, 2015: The JRA-55 Reanalysis: General specifications and basic characteristics. *J. Meteor. Soc. Japan.*, 93, 5-48. https://doi.org/10.2151/jmsj.2015-001

Kohonen, T., 2001. Self-Organizing Maps, Springer Series in Information Sciences. Springer Berlin Heidelberg, Berlin, Heidelberg. https://doi.org/10.1007/978-3-642-56927-2

Lee, H., H. Kim, Y. Honda, Y.-H. Lim, and S. Yi, 2013: Effect of Asian dust storms on daily mortality in seven metropolitan cities of Korea. *Atmos. Environ.*, 79, 510-517. https://doi.org/10.1016/j.atmosenv.2013.06.046

Lee, S., C.-H. Ho, and Y.-S. Choi, 2011: High-PM_{10} concentration episodes in Seoul, Korea: Background sources and related meteorological conditions. *Atmos. Environ.*, 45, 7240-7247. https://doi.org/10.1016/j.atmosenv.2011.08.071

Liang, D., Y.-Q. Wang, C. Ma, and Y.-J. Wang, 2016: Variability in transport pathways and source areas of PM_{10} in Beijing during 2009-2012. *Aerosol Air Qual. Res.*, 16, 3130-3141. https://doi.org/10.4209/aaqr.2016.02.0090

Liu, W., Y. Han, Y. Yin, J. Duan, J. Gong, Z. Liu, and W. Xu, 2018: An aerosol air pollution episode affected by binary typhoons in east and central China. *Atmos. Poll. Res.*, 9, 634-642. https://doi.org/10.1016/j.apr.2018.01.005

Lu, X., C. Lin, Y. Li, T. Yao, J.C.H. Fung, and A.K.H. Lau, 2017: Assessment of health burden caused by particulate matter in southern China using high-resolution satellite observation. *Envorin. Int.*, 98, 160-170, https://doi.org/10.1016/j.envint.2016.11.002

MOE, Ministry of Environment, Korea, 2018: *Annual Report of Air Quality in Korea, 2017*. Korea. https://www.me.go.kr

Nam, J., S.-W. Kim, R.J. Park, J.-S. Park, and S.S. Park, 2018: Changes in column aerosol optical depth and ground-level particulate matter concentration over East Asia. *Air. Qual. Atmos. Health*, 11, 49-60. https://doi.org/10.1007/s11869-017-0517-5

Nandintestseg, B., and M. Shinoda, 2011: Seasonal change of soil moisture in Mongolia: its climatology and modelling. *Int. J. Climatol.*, 31, 1143-1152. https://doi.org/10.1002/joc.2134

Oh, H.-R., C.-H. Ho, J. Kim, D. Chen, S. Lee, Y.-S. Choi, L.-S. Chang, and C.-K. Song, 2015: Long-range transport of air pollutants originating in China: A possible major cause of multi-day high-PM 10 episodes during cold season in Seoul, Korea. *Atmos. Environ.*, 109, 23–30. https://doi.org/10.1016/j.atmosenv.2015.03.005

Park, S.-U., A. Choe, and M.-S. Park, 2013: A simulation of Asian dust events observed from 20 to 29 December 2009 in Korea by using ADAM2. *Asia-Pac. J. Atmos. Sci*., 49, 95-109. https://doi.org/10.1007/s13143-013-0011-4

Penny, S., G.H. Roe, and D.S. Battisti, 2010: The source of the midwinter suppression in storminess over the North Pacific. *J. Climate*, 23, 634-648. https://doi.org/10.1175/2009JCLI2904.1

Qian, W., L. Quan, and S. Shi, 2002: Variations of the dust storm in China and its climatic control. *J. Climate*, 15, 1216-1229. https://doi.org/10.1175/1520-0442(2002)015<1216:VOTDSI>2.0.CO;2

Ryou, H.G., J. Heo, and S.-Y. Kim, 2018: Source apportionment of PM_{10} and $PM_{2.5}$ air pollution, and possible impacts of study characteristics in South Korea. *Environ. Pollut.*, 240, 963-972. https://doi.org/10.1016/j.envpol.2018.03.066

Seo, J. J.Y. Kim, D. Youn, J.Y. Lee, H. Kim, Y.B. Lim, Y. Kim, and H.C. Jin, 2017: On the multiday haze in the Asian continental outflow: the important role of synoptic conditions combined with regional and local sources. *Atmos. Chem. Phys.*, 17, 9311-9332. https://doi.org/10.5194/acp-17-9311-2017

Shao, Y., K.-H. Wyrwoll, A. Chappell, J. Huang, Z. Lin, G.H.M. Tainsh, M. Mikani, T.Y. Tanaka, Z. Wang, and S. Yoon, 2011: Dust cycle: An emerging core theme in Earth system science. *Aeolian Res.*, 2, 181-204. https://doi.org/10.1016/j.aeolia.2011.02.001

Shin, S.-K., D. Muller, C. Lee, K.H. Lee, D. Shin, Y.J. Kim, and Y.M. Noh, 2015: Vertical variation of optical properties of mixed Asian dust/pollution plumes according to pathway of air mass transport over East Asia. *Atmos. Chem. Phys.*, 15, 6707-6720. https://doi.org/10.5194/acp-15-6707-2015

Sun, Y., G. Zhuang, Y. Wang, X. Zhao, J. Li, Z. Wang, and Z. An, 2005: Chemical composition of dust storms in Beijing and implications for the mixing of mineral aerosol with pollution aerosol on the pathway, *J. Geophys. Res.*, 110, D24209, https://doi.org/10.1029/2005JD006054

Takemi, T. and N. Seino, 2005: Dust storms and cyclone tracks over the arid regions in east Asia in spring. *J. Geophys. Res.*, 110, D18S11. https://doi.org/10.1029/2004JD004698

Wang, H.-J. and H.-P. Chen, 2016: Understanding the recent trend of haze pollution in eastern China: roles of climate change. *Atmos. Chem. Phys.*, 16, 4205-4211. https://doi.org/10.5194/acp-16-4205-2016

Wang, L.T., Z. Wei, J. Yang, Y. Zhang, F.F. Zhang, J.Su, C.C. Meng, and Q. Zhang, 2014: The 2013 severe haze over southern Hebei, China: model evalution, source apportionment, and policy implications. *Atmos. Chem. Phys.*, 14, 3151-3173. https://doi.org/10.5194/acp-14-3151-2014

Wang, Y.Q., X.Y. Zhang, J.Y. Sun, X.C. Zhang, X.C. Che, and Y. Li, 2015: Spatial and temporal variations of the concentrations of PM_{10}, $PM_{2.5}$ and PM1 in China. *Atmos. Chem. Phys.*, 15, 13585-13598. https://doi.org/10.5194/acp-15-13585-2015

Wang, Z., X. Pan, I. Uno, X. Chen, S. Yamamoto, H. Zheng, J. Li, and Z. Wang, 2018: Importance of mineral dust and anthropogenic pollutants mixing during a long-lasting high PM event over East Asia. *Environ. Pollut.*, 234, 368-378. https://doi.org/10.1016/j.envpol.2017.11.068

Yu, Y., O.V. Kalashnikova, M.J. Garay, and M. Notaro, 2019: Climatology of Asian dust activation and transport potential. *Atmos. Chem. Phys.*, 19, 363-378. https://doi.org/10.5194/acp-19-363-2019

Zhang, Y., A. Ding, H. Mao, W. Nie, D. Zhou, L. Liu, X. Huang, and C. Fu, 2016: Impact of synoptic weather patterns and inter-decadal climate variability on air quality in the North China Plain during 1980-2013. *Atmos. Environ.*, 124, 119-128. https://doi.org/10.1016/j.atmosenv.2015.05.063

Zheng, S., A. Pozzer, C.X. Cao, and J. Lelieveld, 2015: Long-term (2001-2012) concentrations of fine particulate matter ($PM_{2.5}$) and the impact on human health in Beijing, China. *Atmos. Chem. Phys.*, 15, 5715-5725. https://doi.org/10.5194/acp-15-5715-2015

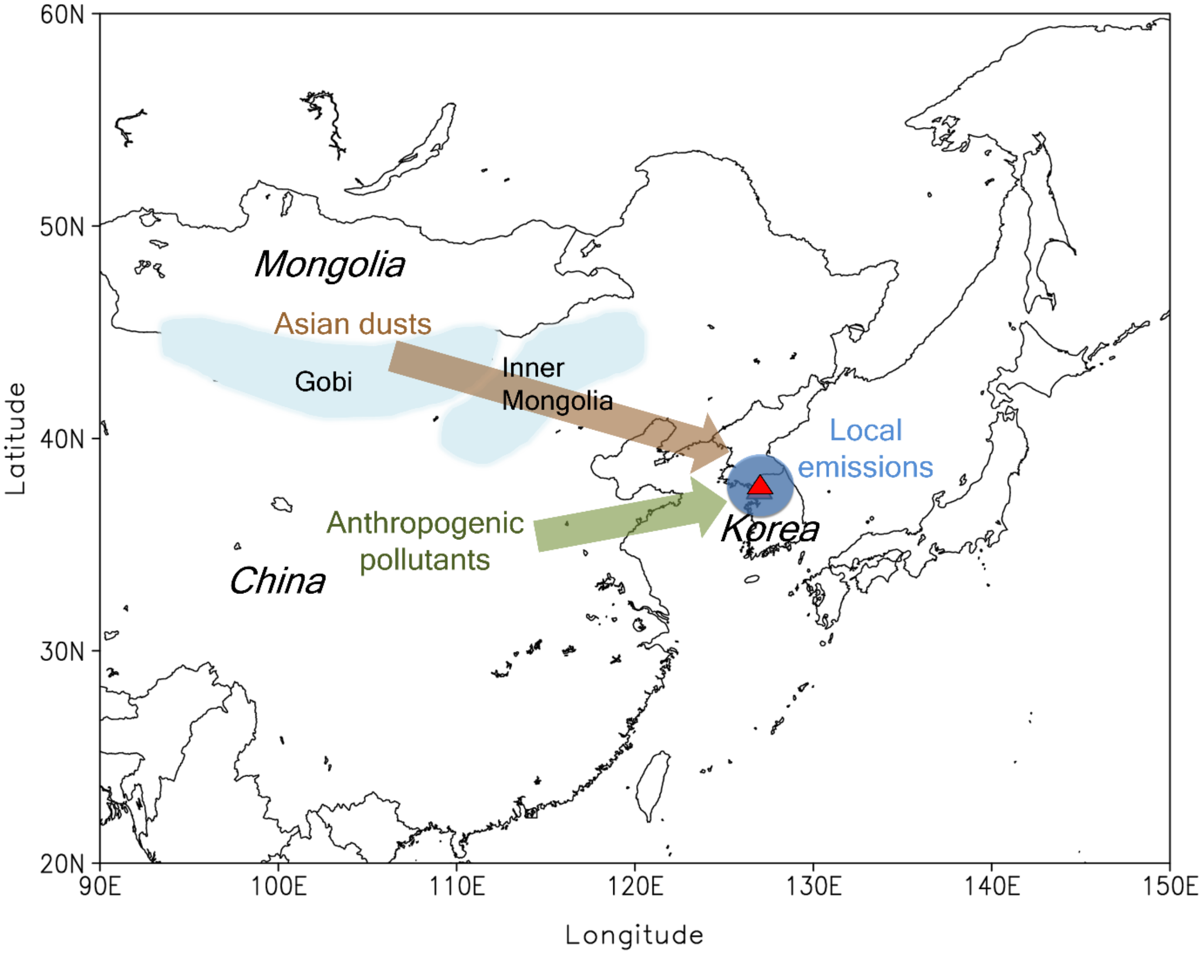

Figure 1. Schematic diagram of the source regions and transport pathways of high PM_{10} concentrations in Seoul, Korea. Desert regions are shaded. The geographical location of Seoul is denoted by the red triangle.

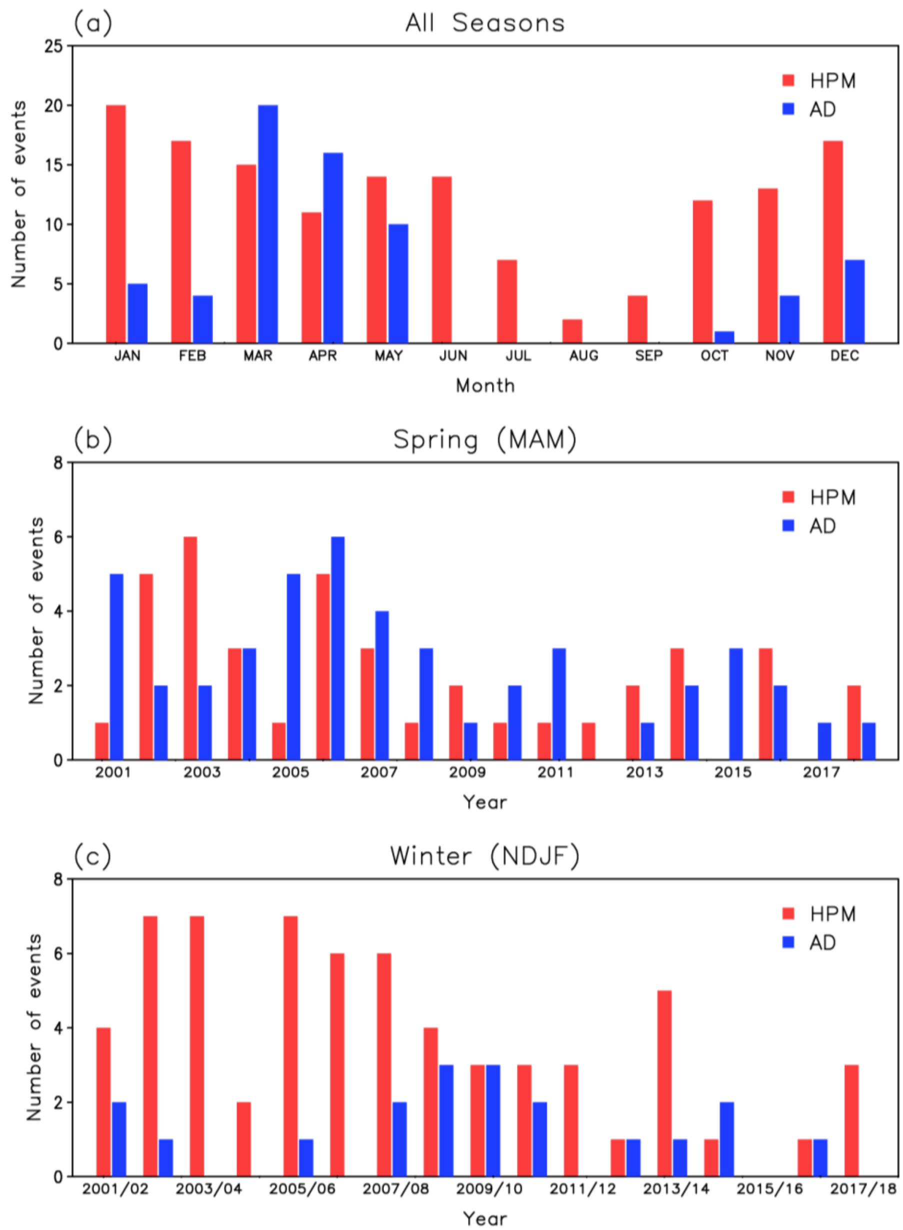

Figure 2. (a) Seasonal cycles of the number of HPM (red) and AD (blue) events in Seoul and (b, c) their changes during (b) MAM and (c) NDJF since 2001.

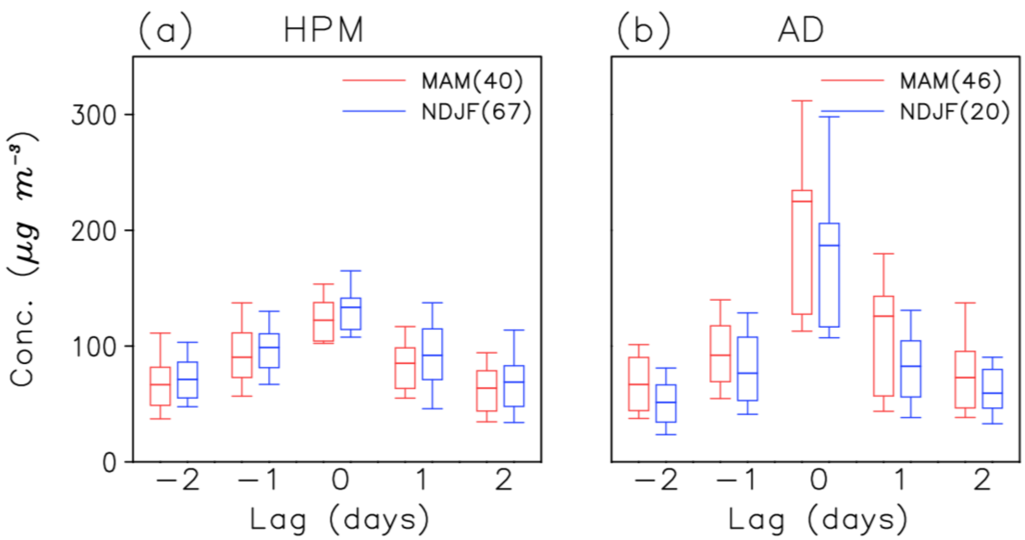

Figure 3. Temporal evolutions of daily-mean PM_{10} concentrations during (a) HPM and (b) AD events in Seoul for MAM (red) and NDJF (blue). Box shows the 75^{th} and 25^{th} percentiles along with the mean value. The bars denote the 90^{th} and 10^{th} percentiles.

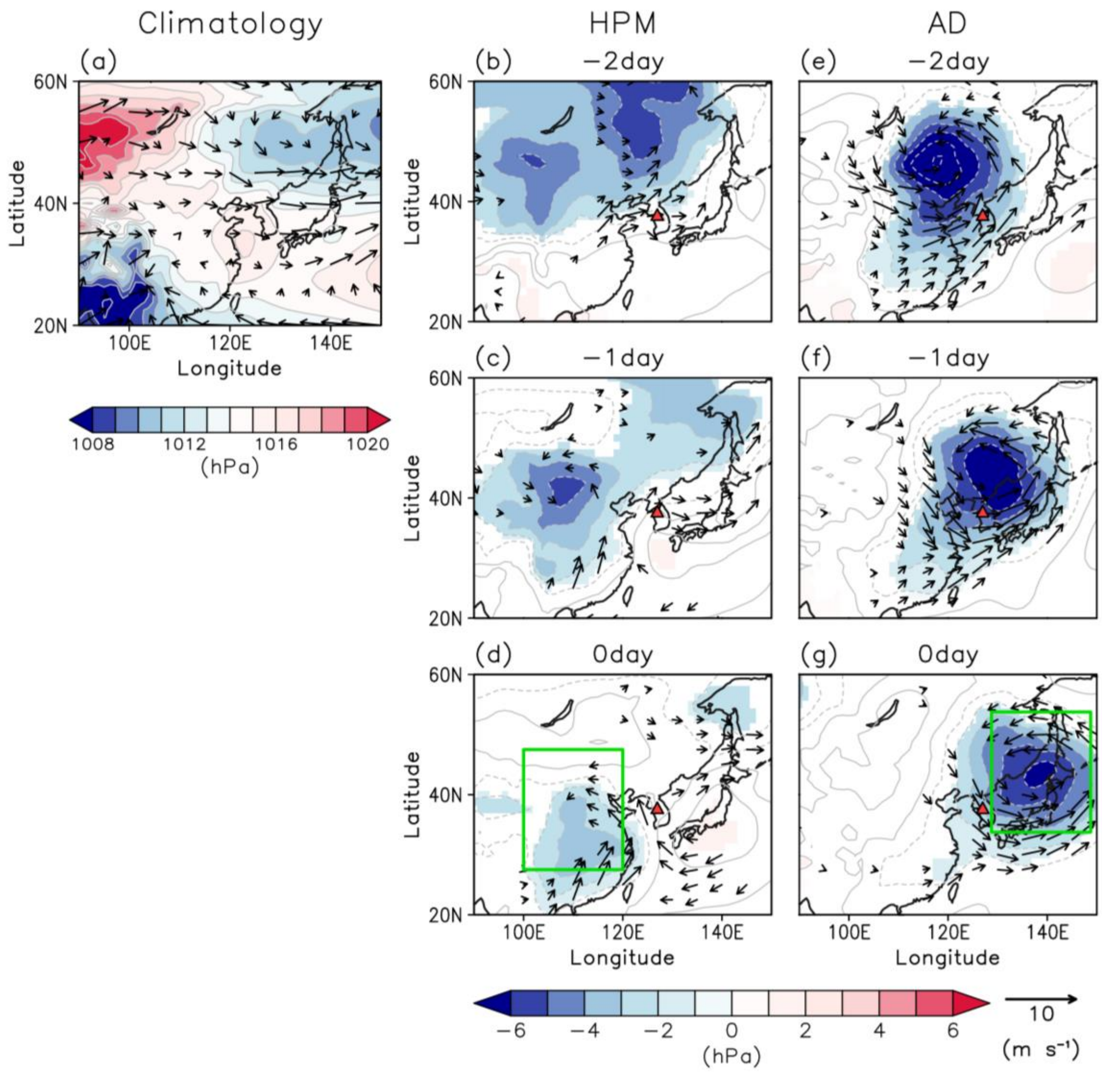

Figure 4. (a) Climatological SLP and 925-hPa wind fields during MAM. (b-g) Composite SLP and 925-hPa wind anomalies from lag -2 to lag 0 days during (left) HPM events and (right) AD events. The shading and black vectors denote statistically significant values at the 95% confidence level. The red triangle indicates the geographical location of Seoul. The green boxes are the analysis domains used in Fig. 7.

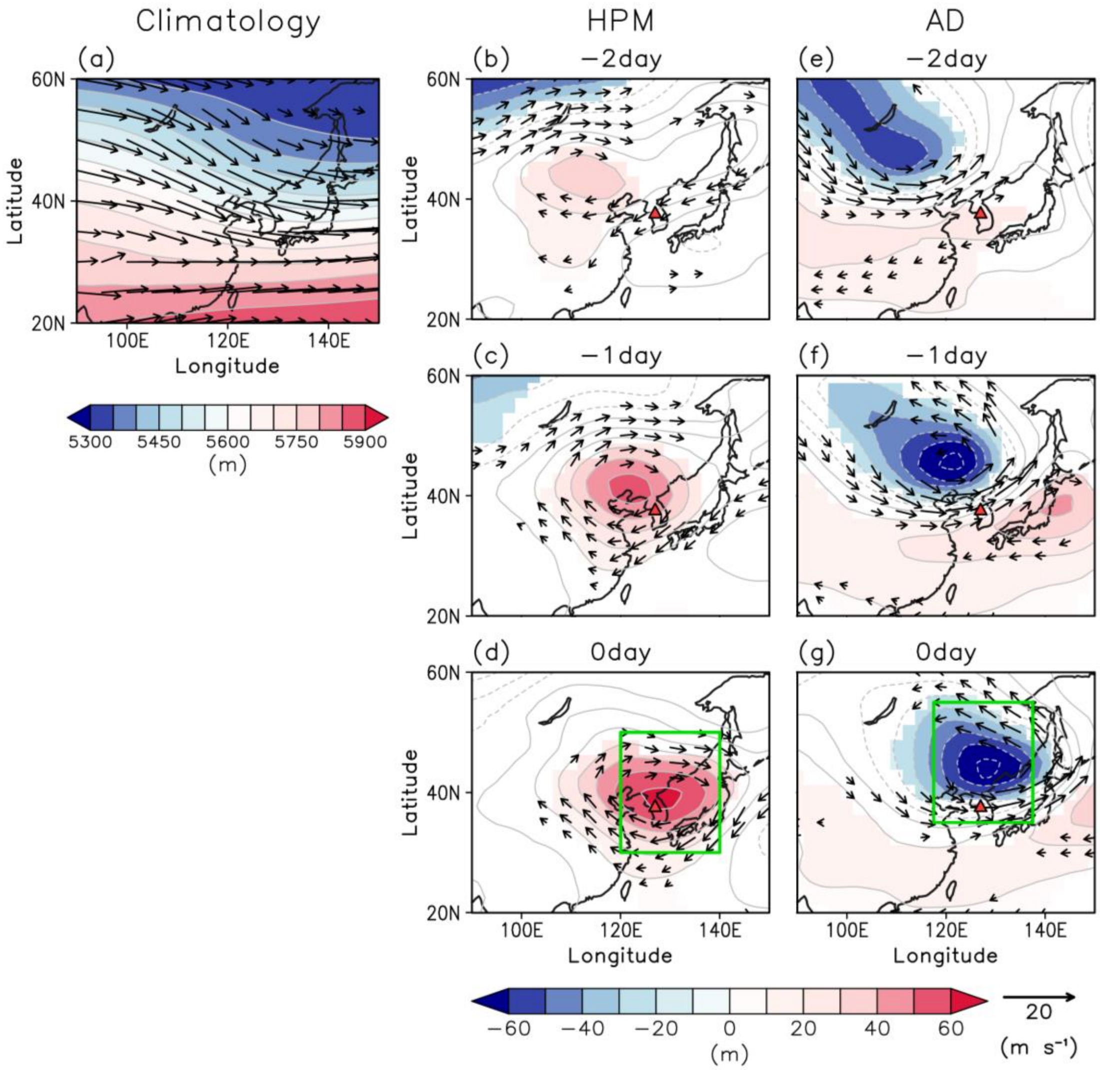

Figure 5. Same as Fig. 4, but for the 500-hPa geopotential height and wind anomalies.

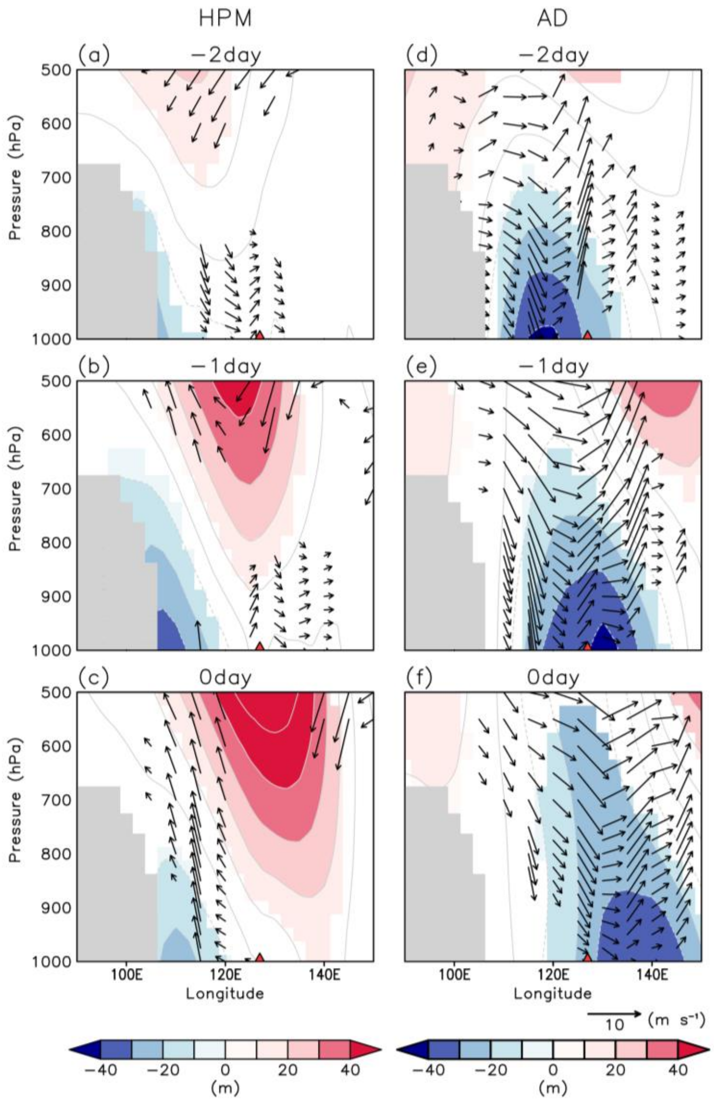

Figure 6. Longitude-pressure cross-section of geopotential height and wind anomalies from lag -2 to lag 0 days during (a-c) HPM and (d-f) AD events. The vector indicates zonal wind and p-velocity anomalies multiplied by the aspect ratio. To represent the vertical motion, the p-velocity sign is reversed. The shading and black arrows denote statistically significant values at the 95% confidence level. The topography is shaded gray.

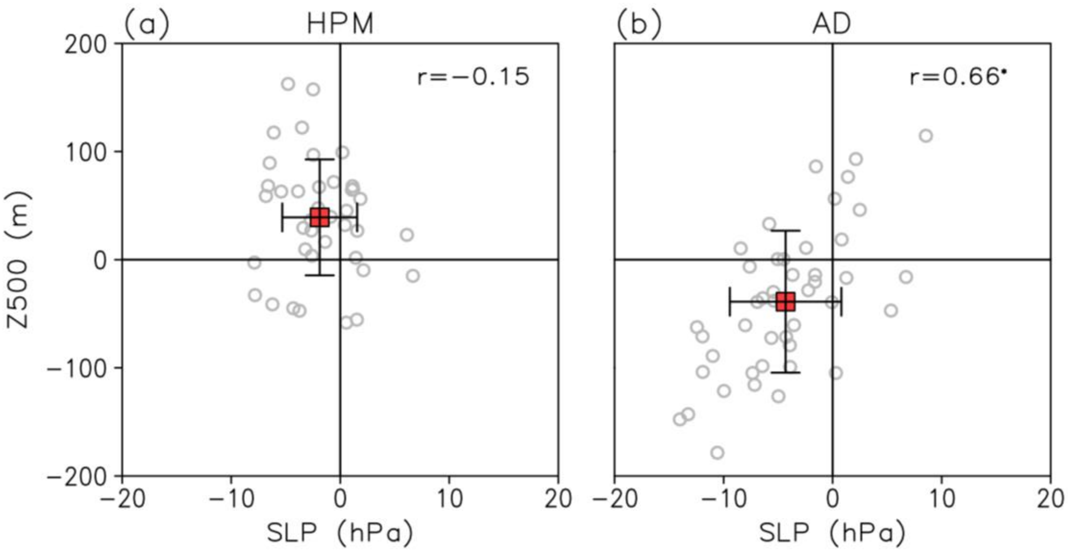

Figure 7. Scatterplot of the area-averaged SLP and 500-hPa geopotential height anomalies for (a) HPM and (b) AD events. The analysis domain used in each plot is denoted by the green boxes in Figs. 4 and 5. Individual events are denoted by gray circles. The mean ± standard deviations are denoted with a red rectangle and error bars. The correlation coefficient, r, that is statistically significant at the 95% confidence level is indicated with an asterisk.

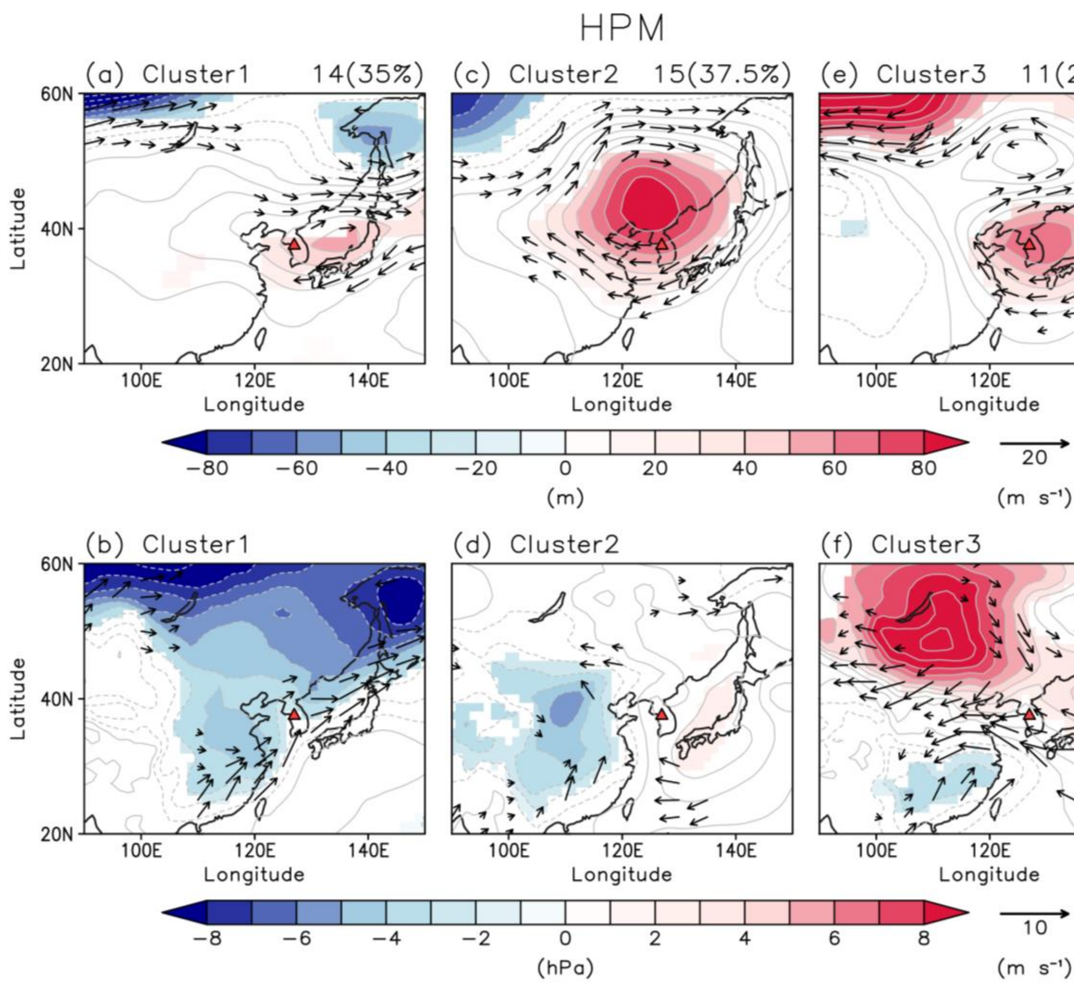

Figure 8. (Top) 500-hPa geopotential height and wind anomalies on the central date of HPM events for each cluster. (Bottom) Same as top panels but for the SLP and 925-hPa wind anomalies. The number of events and proportion of each cluster are indicated in the subtitle. Values that are statistically significant at the 95% confidence level are shaded.

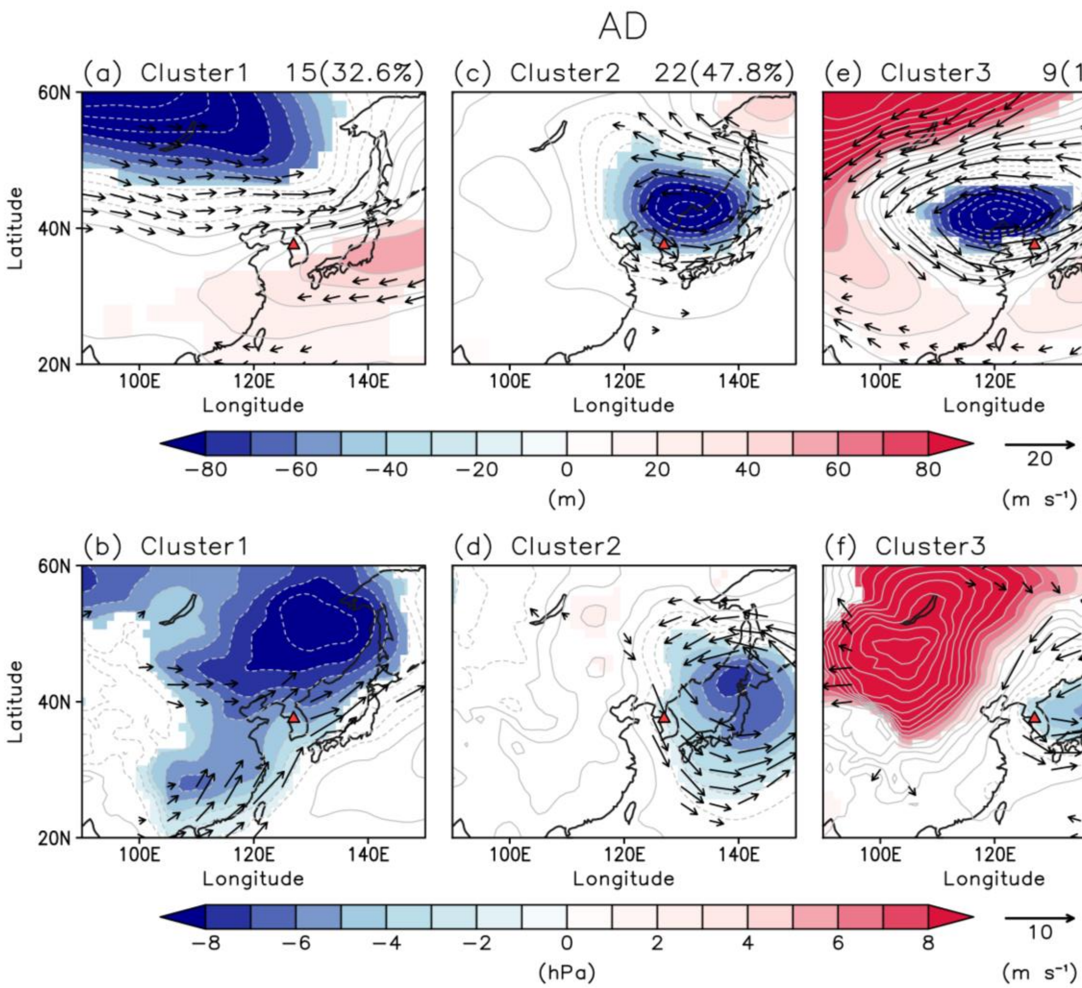

Figure 9. Same as Fig. 8, but for AD events.